

RECONSTRUCTING LATE HOLOCENE FLOOD RECORDS IN THE TYWI CATCHMENT

Final report for
Dyfed Archaeological Trust
for the Exploration Tywi! Project.

February 2011

**Anna F. Jones, Paul A. Brewer, Mark G. Macklin
and Catherine. H. Swain**

Centre for Catchment and Coastal Research
Institute of Geography and Earth Sciences
Aberystwyth University
Aberystwyth
SY23 3DB

List of Figures

Figure 1	The Tywi catchment, south Wales, showing the locations of the Exploration Tywi! study area, the principal towns, the three gauging stations and the Abermarlais field site.	4
Figure 2	Annual maximum series derived from daily mean flow data and HiFlows-UK data for the Dolau Hirion flow gauge	6
Figure 3	Annual maximum series derived from daily mean flow data, daily maximum flow data and data from the HiFlows-UK archive for the Ty Castell flow gauge.	8
Figure 4	Annual maximum series derived from daily mean flow data, daily maximum flow data and data from the HiFlows-UK archive for the Capel Dewi flow gauge.	8
Figure 5	Temporal variations in the magnitude of the annual maximum flood at Dolau Hirion.	11
Figure 6	Temporal variations in the magnitude of the annual maximum flood at Ty Castell.	12
Figure 7	Temporal variations in the magnitude of the annual maximum flood at Capel Dewi.	14
Figure 8	Variations in the winter (December-March) North Atlantic Oscillation index between 1900 and 2009.	16
Figure 9	Flood frequency analysis of annual maximum flood data from the Dolau Hirion gauging station.	17
Figure 10	Flood frequency analysis of annual maximum flood data from the Ty Castell gauging station.	19
Figure 11	Flood frequency analysis of annual maximum flood data from the Capel Dewi gauging station.	20
Figure 12	Geomorphological map of the Abermarlais site, showing the locations of the cores (AM C1 and AM C3).	31
Figure 13	The most significant positive correlation between the log-ratio of Zr/Ti and sediment grain size (the ratio of the 5.5-6.0 ϕ fraction to the 9.5-10.0 ϕ fraction).	38
Figure 14	The most significant positive correlation between the log-ratio of Zr/Rb and sediment grain size (the ratio of the 5.5-6.0 ϕ fraction to the 9.5-10.0 ϕ fraction).	38

List of Tables

Table 1	Record lengths of available daily mean flow, daily maximum flow and HiFlows-UK annual maximum series for the selected flow gauges.	9
Table 2	Historical flood events in the Tywi catchment.	27
Table 3	Pearson product-moment correlation between grain-size log-ratios calculated using data from the Sedigraph and Zr/Ti log-ratios for the 16 subsamples from the Abermarlais cores).	35
Table 4	: Pearson product-moment correlation between grain-size log-ratios calculated using data from the Sedigraph and Zr/Rb log-ratios for the 16 subsamples from the Abermarlais cores.	36
Table 5	Pearson product-moment correlation between grain-size log-ratios calculated using data from the laser granulometer and Zr/Ti log-ratios for the 16 subsamples from the Abermarlais cores.	39
Table 6	Pearson product-moment correlation between grain-size log-ratios calculated using data from the laser granulometer and Zr/Rb log-ratios for the 16 subsamples from the Abermarlais cores.	40

1. To establish the recent history of flooding, and of variations in flood magnitude, through analysis of instrumental flood records;
2. To describe the methods used in reconstructing long flood records from floodplain sedimentary sequences;
3. To demonstrate that the grain size proxies employed are suitable for use at the study sites;
4. To produce long dated flood records from floodplain sediment sequences within the Tywi catchment, which can be used to investigate relationships between flooding and climate;
5. To compare the sedimentary flood record with available historical flood records, in terms of length and type and utility of the information provided.

1.3 Structure of the report

This report consists of six sections, including this introduction. Section 2 describes the Tywi catchment and site investigated as part of this research. Section 3 presents flow data from three gauging stations within the Tywi catchment. Recent (decadal-scale) variations in flood magnitude are described and their effects on the results of flood frequency analysis are assessed. Section 4 summarises the available historical flood data for the Tywi catchment. Section 5 presents flood records constructed using high-resolution Itrax core scanning of sedimentary sequences from Abermarlais. Section 6 summarises the main findings of the study and suggests lines of enquiry for further research.

2. The Tywi catchment and Abermarlais study site

The Afon Tywi, in south-west Wales, is 114 km in length and has a catchment area of 1373 km². The catchment rises to 802 m above Ordnance Datum in Black Mountain, on its southern boundary. The catchment is predominantly underlain by mudstones, siltstones and greywackes of Ordovician and Silurian age but at the southern margin of the catchment Devonian sandstones (Old Red Sandstone) and Carboniferous limestone crop out. Grassland, used either for hill-farming, livestock farming or dairying, is the predominant land cover type within the catchment and there is also a significant proportion of woodland. Arable land and urban areas constitute relatively small percentages of catchment land cover.

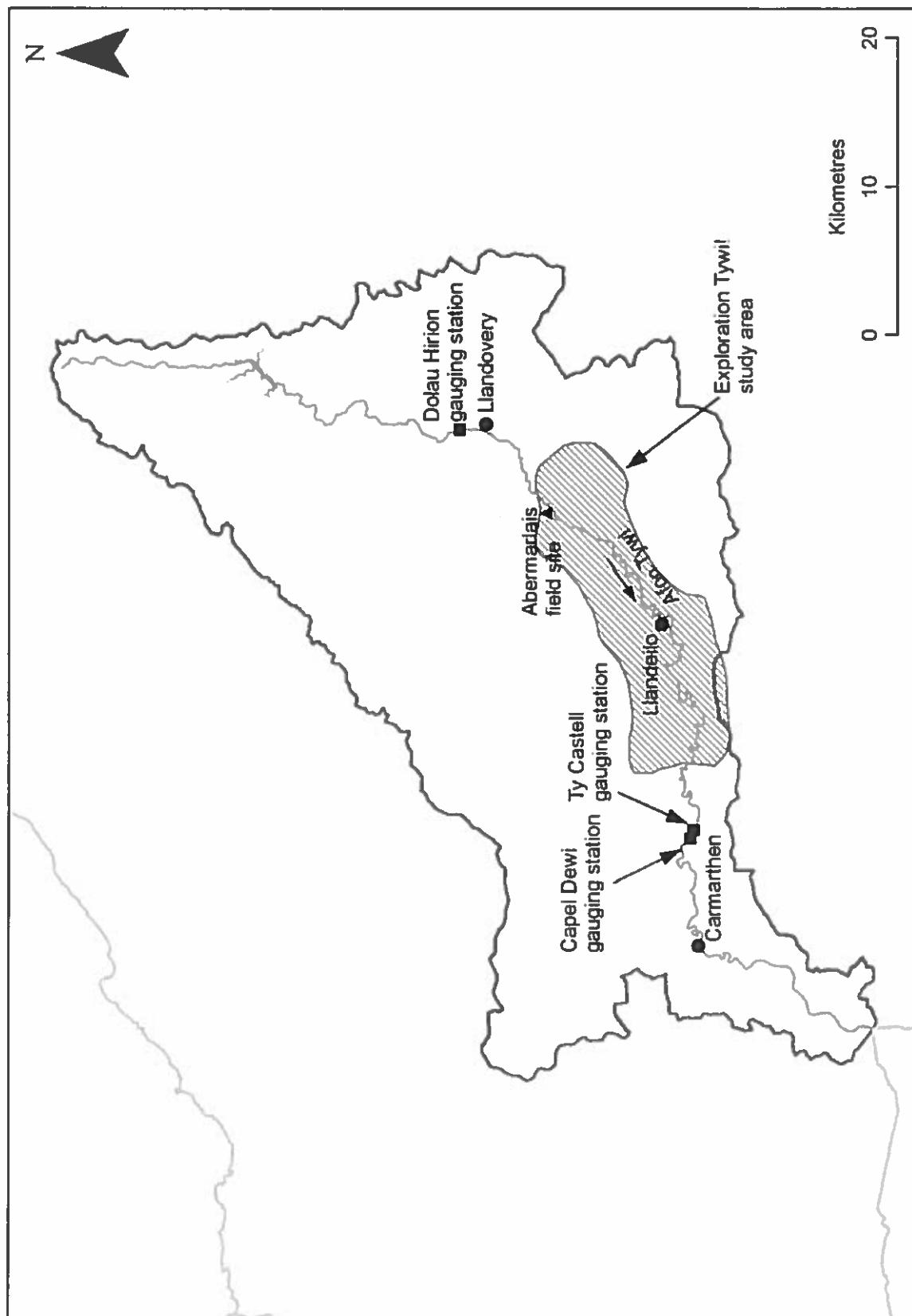


Figure 1: The Tywi catchment, south Wales, showing the locations of the Exploration Tywi! study area, the principal towns, the three gauging stations and the Abermarlais field site.

Table 1: Record lengths of available daily mean flow, daily maximum flow and HiFlows-UK annual maximum series for the selected flow gauges.

	Dolau Hirion	Ty Castell	Capel Dewi
Gauging station established	25/04/1968	01/01/1958	01/02/1958
Daily mean flows (water years)	1968-2008	1958-1983 and 1999-2009	1974-2009
Daily maximum flows (water years)	No record	1981-1983 and 1999-2009	1981-2009
HiFlows-UK annual maximum data (water years)	1967-2007	1957-2007	1957-2007*

* HiFlows-UK data for 1957-1973 water years at Capel Dewi have been derived from data from the Ty Castell gauge (Environment Agency, 2010).

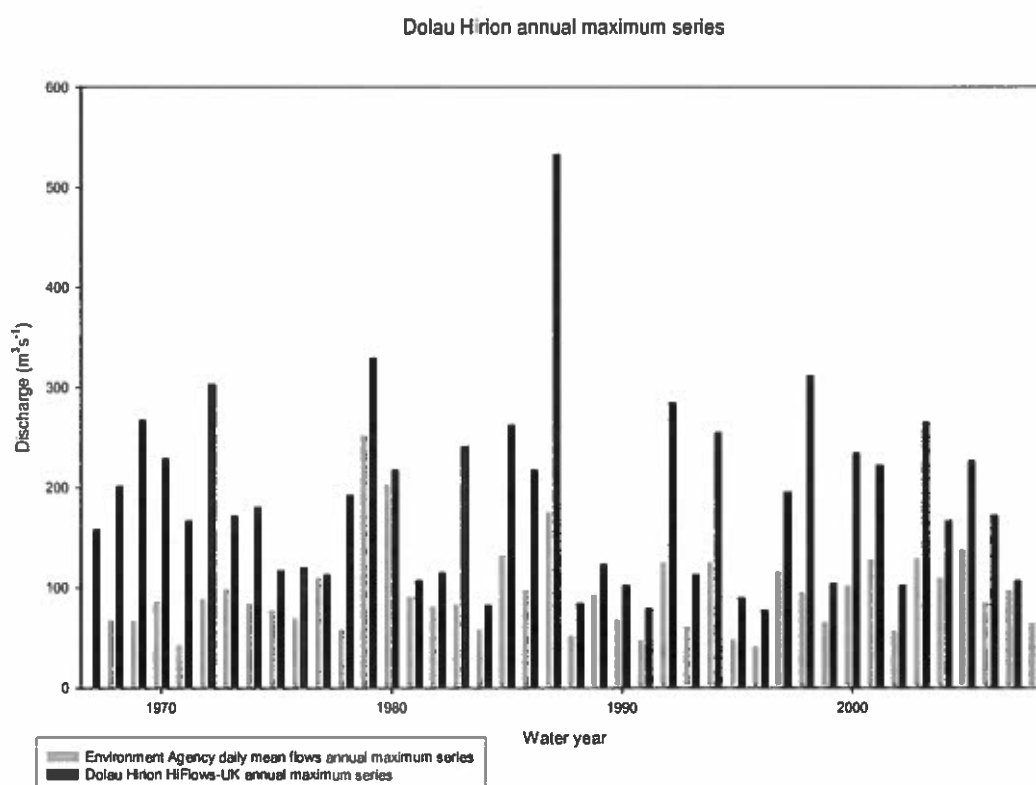


Figure 2: Annual maximum series derived from daily mean flow data and HiFlows-UK data for the Dolau Hirion flow gauge.

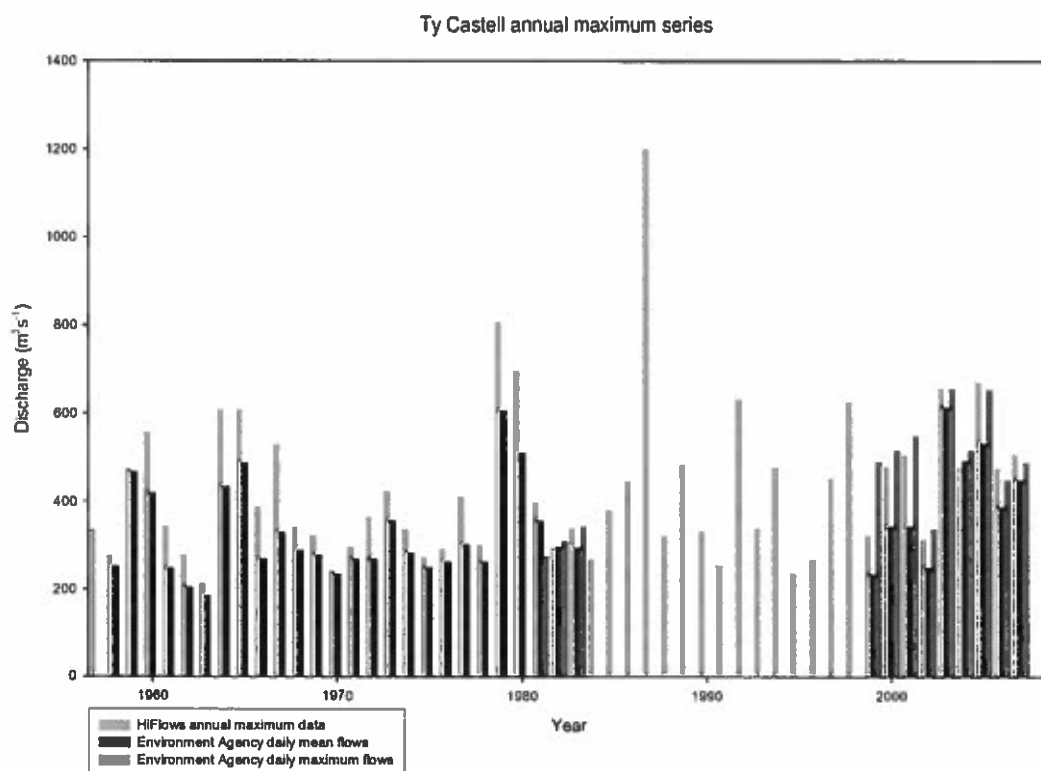


Figure 3: Annual maximum series derived from daily mean flow data, daily maximum flow data and data from the HiFlows-UK archive for the Ty Castell flow gauge.

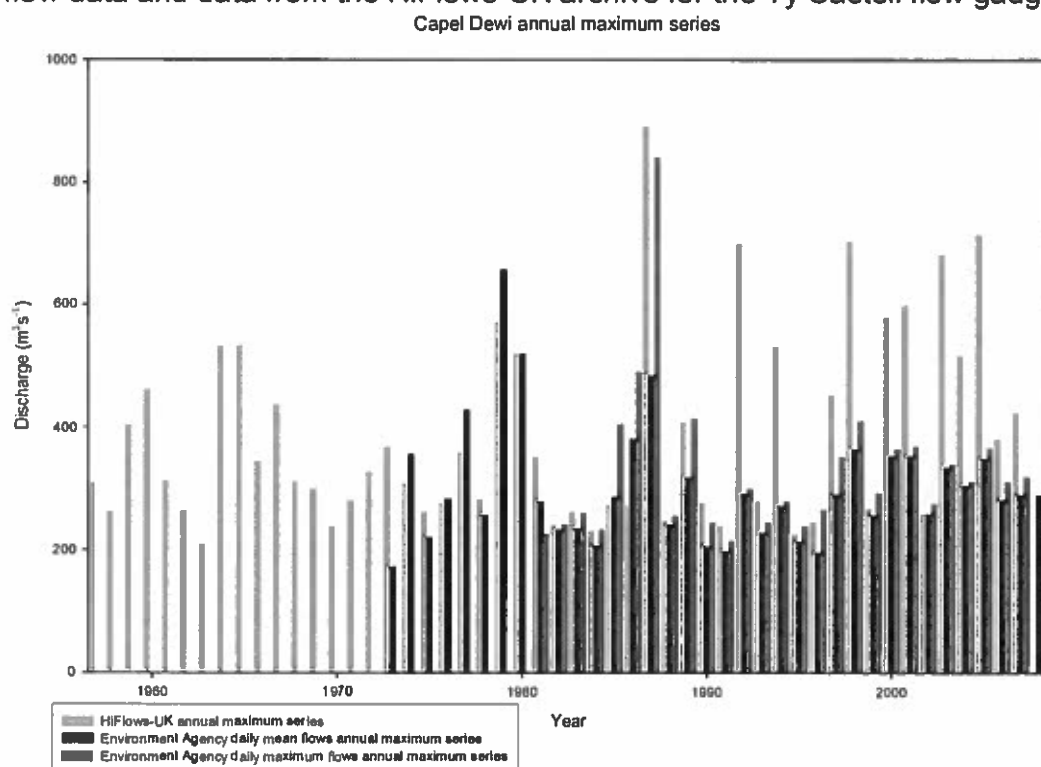


Figure 4: Annual maximum series derived from daily mean flow data, daily maximum flow data and data from the HiFlows-UK archive for the Capel Dewi flow gauge. 1987 ($175 \text{ m}^3 \text{s}^{-1}$) respectively, whereas in the HiFlows-UK annual maximum flood

difference in the magnitude of the annual maximum flood discharges between the two datasets is striking: in the daily mean flow data the largest flood peak is a little over $250 \text{ m}^3\text{s}^{-1}$ while in the HiFlows-UK data the magnitude of the greatest annual maximum flood peak is in excess of $500 \text{ m}^3\text{s}^{-1}$. In this small, rapidly responding upland catchment it appears that there may be large differences between daily mean and maximum flows.

At the Ty Castell gauge there are long gaps (1984-1998) in the annual maximum flood records derived from both the daily mean and daily maximum flow records, which make it difficult to identify temporal variations in the magnitude of the annual maximum flood. The short record derived from the daily maximum flow series shows that the greatest annual maximum flood peaks occurred in the 2003 and 2005 water years. The flood peaks recorded in the 1981-1983 water years are smaller than the majority of those which occur during the period 1999-2009. The annual maximum flood record derived from the daily mean flow series contains a peak in the early part of the record with the greatest annual maximum flood event occurring in the 1965 water year.

Relatively low annual maximum flood peaks were recorded during the early to mid 1970s followed by an increase to a peak in 1979-1980. In the most recent part of the record there is a peak at c. 2003-2005, corresponding to that in the daily maximum flow record. The HiFlows-UK record is the only one which covers the entire period and this indicates that the annual maximum flood event in the 1987 water year dwarfs every other annual maximum flood discharge in the record. The pattern of variation in the early part of the record is similar to that in the annual maximum series derived from the daily mean flow record, although the magnitude of the instantaneous maximum discharges is $100\text{-}200 \text{ m}^3\text{s}^{-1}$ greater for the larger events in this period. The later part of the record shows a similar pattern to that recorded at Dolau Hirion, namely a decrease in mean annual maximum flood magnitudes to the early to mid 1990s followed by an increase to the end of the record.

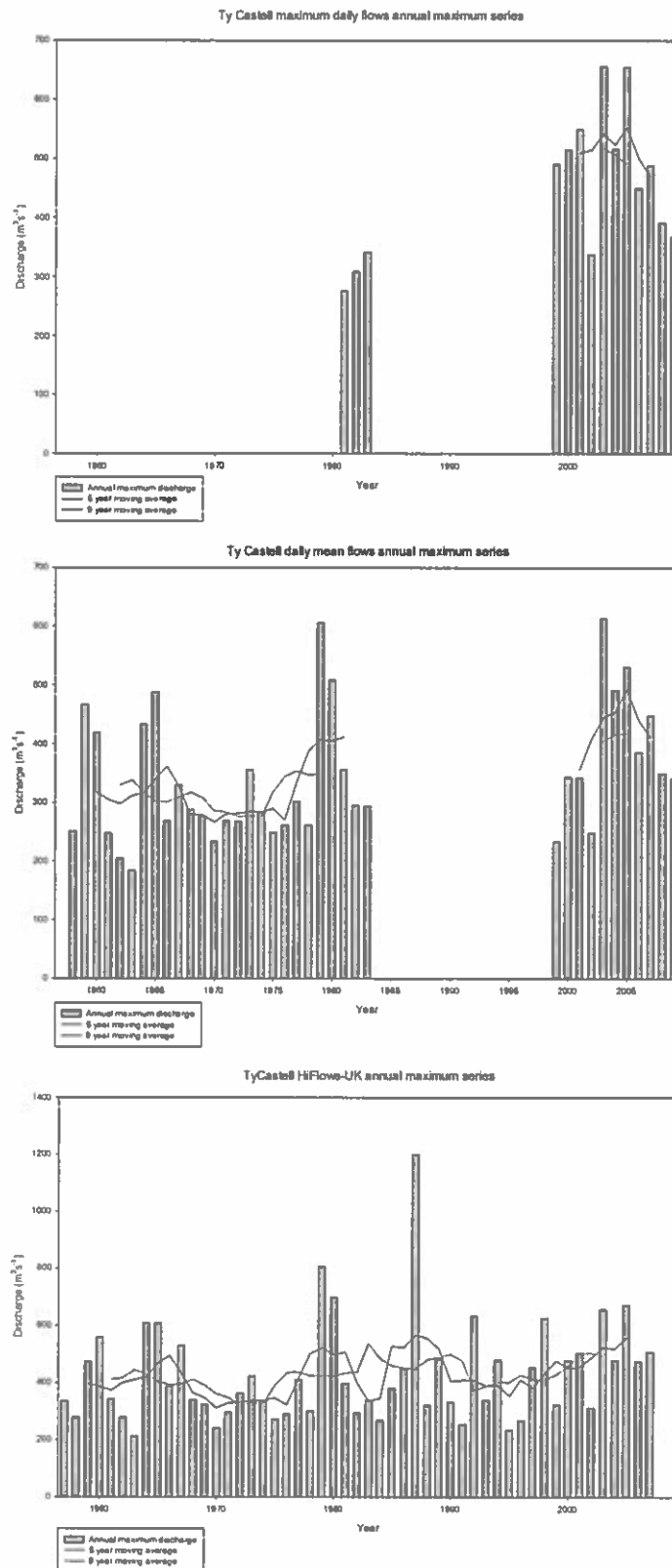


Figure 6: Temporal variations in the magnitude of the annual maximum flood at Ty Castell. Flood magnitudes are derived from daily maximum flow data (top), daily mean flow data (middle) and the HiFlows-UK archive (bottom).

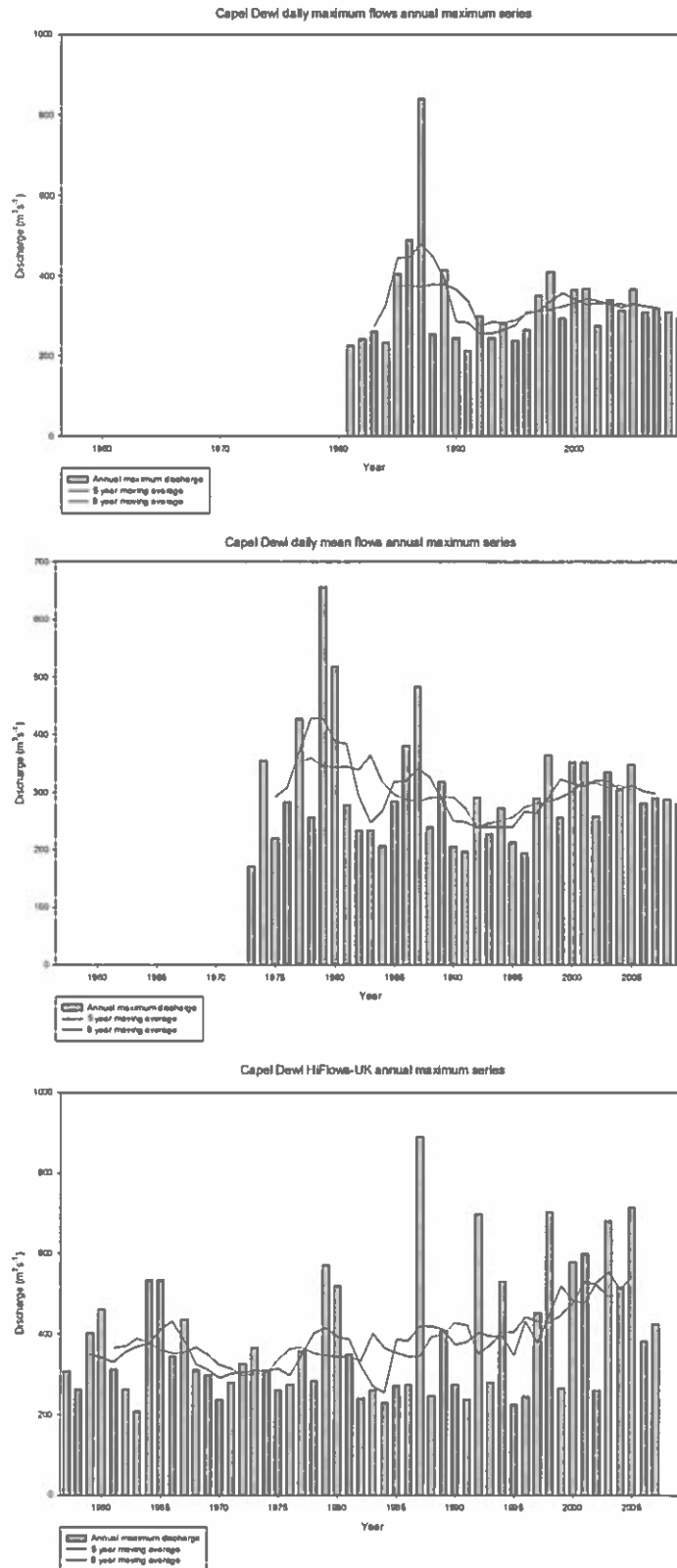


Figure 7: Temporal variations in the magnitude of the annual maximum flood at Capel Dewi. Flood magnitudes are derived from daily maximum flow data (top), daily mean flow data (middle) and the HiFlows-UK archive (bottom).

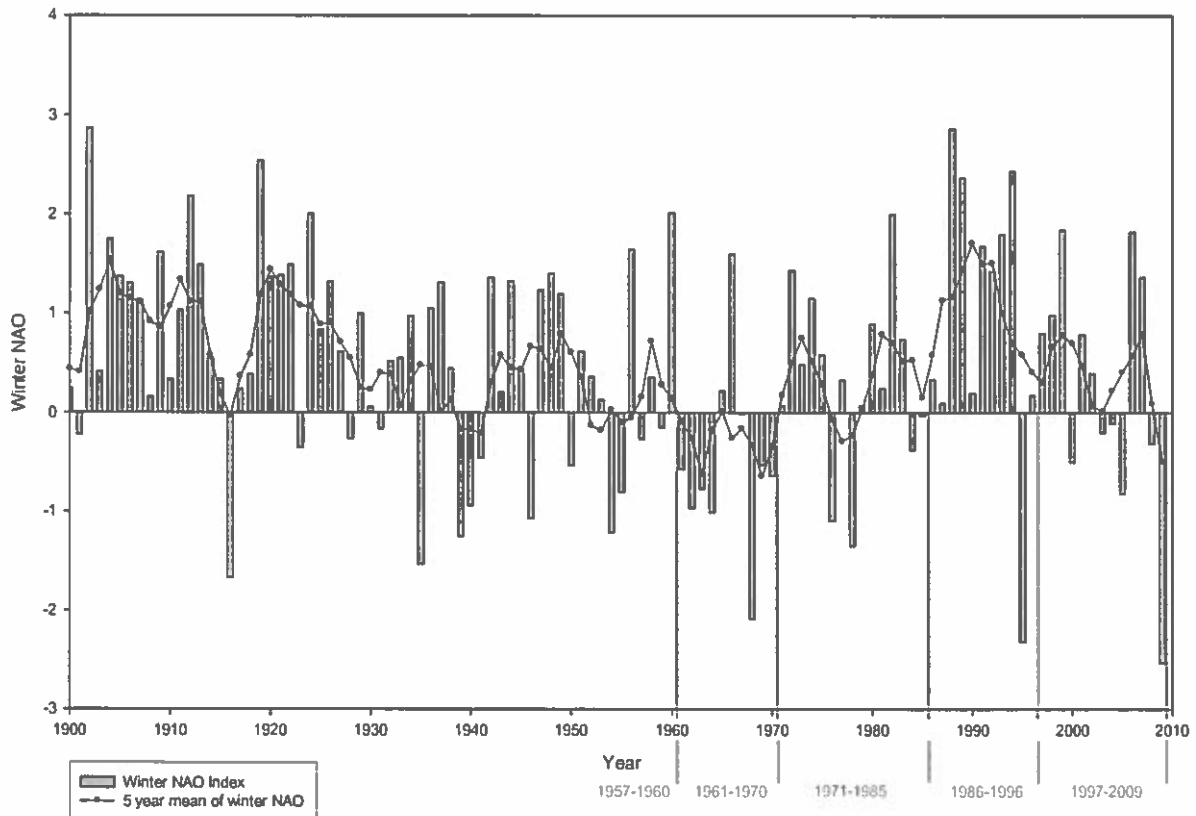


Figure 8: Variations in the winter (December-March) North Atlantic Oscillation index between 1900 and 2009. The data have been smoothed using a 5-year running mean which has been used to define five periods (below right) into which the annual maximum flood records have been divided for flood frequency analysis.

one year in 20 through the whole record. This rises to more frequently than one year in ten during the 1971-1985 period as a result of the occurrence of the two highest mean daily flows during this period. The results from the analysis of the HiFlows-UK annual maximum data are somewhat different: in each data series, except that for the 1967-1970 water years, there is a noticeable step change in the magnitudes of the annual maximum floods as the exceedence probability decreases. This occurs at between c. 70 % and 40 % annual exceedence probabilities, depending on which part of the record is analysed. This effect may result from the operation of the Llyn Brianne to contain flood flows when floodwater storage capacity is available. In the whole record the apparent reduction in flows which may be due to the operation of the reservoir occurs for floods with exceedence probabilities greater than c. 60 %. The HiFlows-UK instantaneous maximum data indicate that annual maximum flood peaks exceed $300 \text{ m}^3\text{s}^{-1}$ approximately one year in ten.

The probability of such an event occurring appears elevated in the 1971-1985 and 1986-1996 periods, notably as a result of the occurrence of the single high-magnitude flood in 1987 for the 1986-1996 period. As in the flood frequency analysis on the daily mean flow data, frequent floods in the 1986-1996 period had substantially lower flood peak discharges than those in other parts of the record.

Flood frequency analysis of the small amount of daily maximum flow data from the Ty Castell gauge emphasises the lower magnitude of the flood peaks in the 1981-1983 water years as compared with those between 1999-2009. The analysis of the daily mean data indicate that flood magnitudes were generally lower in 1971-1983 and 1961-1970 than in 1999-2009, although magnitudes of the floods with the lowest annual exceedence probabilities in 1971-1983 and 1999-2009 are very similar. Flood frequency analysis of the HiFlows-UK data for this gauge emphasises the high magnitude of the 1987 flood peak. Through much of the range of annual exceedence probabilities, flood magnitudes were greater in the 1997-2007 than in the other parts of the record. In the entire record the magnitude of the flood which occurs on average in one year in ten was approximately $650 \text{ m}^3\text{s}^{-1}$. This value varied from between $608 \text{ m}^3\text{s}^{-1}$ for the 1961-1970 period to c. $1000 \text{ m}^3\text{s}^{-1}$ in the 1986-1996 period, as a result of the high magnitude of the 1987 annual maximum flood, which, according to the flood frequency analysis on the whole records, would be expected to occur in around one year in 50.

Flood frequency analysis of the annual maximum flood record derived from maximum daily flow data at the Capel Dewi gauge shows that high-magnitude flood events, with low annual exceedence probabilities, were most frequent in the 1986-1996 period. For events with higher annual exceedence probabilities, magnitudes were greater during the 1997-2009 period than in either 1981-1985 or 1986-1996. This is also apparent in the flood record derived from daily mean flow data. However, for floods with low annual exceedence probabilities, the annual maximum flood record derived from the mean daily flow data indicates that the magnitudes of such flows were greatest during the 1973-1985 period. The flood frequency analysis on the data from the HiFlows-UK data from the Capel Dewi gauge produces different results. Flood magnitudes are greatest in the 1997-2007 period for floods with annual exceedence probabilities of between 10 and 80 %. As at the Ty Castell gauging station the magnitudes of floods with annual exceedence probability of 10 % vary considerably between different parts of the record, being greatest in 1986-1997 and least in 1961-1970.

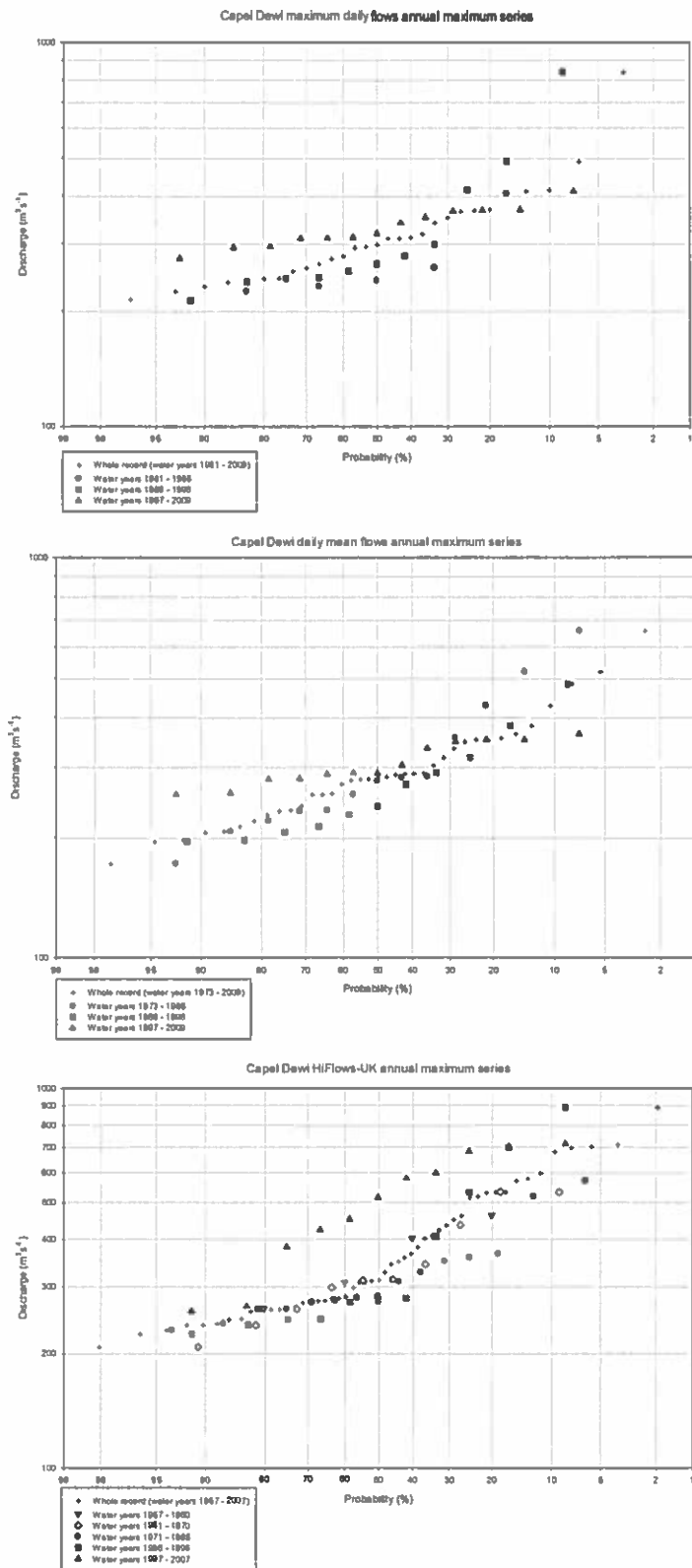


Figure 11: Flood frequency analysis of annual maximum flood data from the Capel Dewi gauging station. Flood magnitudes are derived from daily maximum flow data (top), daily mean flow data (middle) and the HiFlows-UK archive (bottom).

4. Historical flood data

4.1 Introduction

In the previous section the systematically collected instrumental flow record was the subject of investigation. In this section the potential of the available historical data for extending the instrumental record is assessed for the Tywi catchment.

4.2 Historical flood data for the Tywi catchment

Historical flood data for the Tywi catchment have been obtained from the Chronology of British Hydrological Events database (CBHE) (Black and Law, 2004; Law *et al.*, 1998), which contained data from a range of sources. In addition, quantitative information for a single flood event which occurred prior to gauging of flows within the catchment is available from the Flood Studies Report (NERC, 1975). It is noted that information on certain floods obtained from the CBHE has since been removed from the database. No reason for this removal has yet been ascertained. However, much of the removed data had been extracted from a published source (Lewis, 1992) and is therefore included in this assessment of the available historical data.

Table 2 lists the dates of the flood events which are referred to in historical sources and also includes available information on flood magnitude. The available information suggests that the record is incomplete for the period from 1767: there are probably one or more floods of greater magnitude than that of 1831 which occurred during the 50 years prior to that date. Likewise, there is no record of the flood of 1852, although the information about the flood of 1878 imply that the flood peak magnitude in 1852 was greater than that in 1878. In addition, there is no information about the snowmelt flooding which occurred in March 1947. The only flood for which quantitative information is available is that of 1931 for which a discharge of $1270 \text{ m}^3\text{s}^{-1}$ has been estimated, putting the peak discharge of this event close to that of the high-magnitude flood of 1987, which was the largest, by a significant margin, in the instrumental flow record.

Frost and Jones (1988) concluded that the peak discharge of the flood event of 1894 may have been greater than any flood in the instrumental record (including that of 1987), while the information collected by Lewis (1992) indicates that the flood peak discharge of the 1891 event may only have been a little lower than that of 1894. These data suggest that, since c. 1890 four flood events with a discharge similar to that of the flood of 1987 (including the 1987 flood itself) may have occurred. For those events which occurred prior to 1891 the information on flood magnitude is too limited to draw any conclusions about the length of time during which the discharges of the floods of 1891 and 1894 had not been exceeded.

4.3 Usefulness of historical flood data

Quantitative historical data, such as the estimated discharge for the 1931 at Ty Castell, are clearly the most useful for extending the instrumental flood record, particularly where rating equations exist which are suitable for converting high-magnitude flood stages to discharges. Relative magnitude information (flood X > flood Y or flood Z the largest for W years) may also potentially be incorporated into estimates of annual exceedence probabilities (cf. palaeohydrologic bounds (Levish, 2002)) where appropriate statistical techniques are available. Where magnitude data are lacking, information that a significant flood has occurred may be of use in constraining flood frequencies, although it will not be possible to attach a frequency to a particular magnitude as in conventional flood frequency analysis.

Historical flood peak data may also be used in conjunction with palaeoflood data to extend flood records. Dates of significant flood events and relative magnitudes of numbers of flood events may be used to identify events within the palaeoflood record. The dating of these events within the palaeoflood record becomes particularly secure when other dating control (for instance from radiocarbon or historical contamination) is available. Where event magnitudes are available within the historical record, floods within the palaeoflood record which occurred prior to historical recording of flood levels may be classified as having peak magnitudes 'probably greater than flood X' or 'probably less than flood Y'. This type of information may also be useful in constraining the magnitude-frequency relationships of high-magnitude flood events with low annual exceedence probabilities. The type of palaeoflood information derived from floodplain sedimentary sequences, as described in the following section, is particularly suitable for

1992), degree of trace element enrichment (e.g. Shotyk *et al.*, 2001; Wolfe and Härtling, 1997), depositional process (e.g. Thorndycraft *et al.*, 1998) and grain size (e.g. Calvert *et al.*, 2001; Chen *et al.*, 2006; Dypvik and Harris, 2001; Oldfield *et al.*, 2003).

In a lacustrine sedimentary sequence from Petit Lac d'Annecy, France, Thorndycraft *et al.* (1998) were able to identify four major flood events using changes in the Fe/Mn ratio within the core: significantly higher values of the Fe/Mn ratio resulted from the high Fe content of minerogenic soils washed into the lake during these events. Since discrimination of flood events in fluvial sedimentary sequences is usually undertaken primarily upon the basis of grain size reversals, element ratios indicative of changes in grain size offer the potential for distinguishing between the deposits of individual flood events in fine-grained sedimentary sequences. The combination of element ratios indicative of sediment grain size changes and high-resolution core scan data provides the capability for reconstructing highly detailed records of past flood events from fluvial sedimentary sequences lacking clearly visible sediment grain size reversals.

A number of lithogenic element ratios have been used as indicators of changing grain size in various types of sediment including Si/Al (e.g. Calvert *et al.*, 1996; Calvert *et al.*, 2001), Ti/Al (e.g. Calvert *et al.*, 1996; Schneider *et al.*, 1997), Zr/Al (e.g. Calvert *et al.*, 2001; Schneider *et al.*, 1997), Zr/Ti (Oldfield *et al.*, 2003) and Zr/Rb (Chen *et al.*, 2006; Dypvik and Harris, 2001). The poor detection limits of Al and Si in Itrax XRF analyses (approximately 20 000 ppm and 10 000 ppm, respectively, using a 10 second count time; Cox Analytical Systems (no date)) means that ratios incorporating these elements were unsuitable for interpreting grain size changes from Itrax XRF data. For this reason, the application of the Zr/Ti and Zr/Rb ratios in palaeoflood reconstruction was investigated in this study.

Zr, Ti and Rb are lithogenic elements (Oldfield *et al.*, 2003; Shotyk *et al.*, 2001) which have been used as indicators of catchment erosion in lake sediment studies (e.g. de Boer, 1997; Koinig *et al.*, 2003; Wolfe *et al.*, 2005). Zr is immobile in the surficial environment (Hardardóttir *et al.*, 2001; Law *et al.*, 1991; Rose *et al.*, 1979), while Rb is slightly mobile (Rose *et al.*, 1979). Ti is often considered immobile (Hardardóttir *et al.*, 2001; Rose *et al.*, 1979), although mobility of Ti has been reported during weathering of soils, when it becomes enriched in the clay fraction (Sudom and St. Arnaud, 1971). Zr is generally insoluble (Koinig *et al.*, 2003) whereas Ti has low solubility in low temperature

(median 2.92 %) and 63-125 μm (median 2.54 %) fractions of 121 bed sediment samples from Manoa Stream, Hawaii. Veldkamp and Kroonenberg (1993) studied the effect of grain size on the composition of sandy sediment from river terraces in the Allier and Dore catchments in the Limagne rift valley, France. They found that grain size had a significant effect on the concentration of Rb in the Allier catchment (higher Rb, lower median grain size over the range 0.2- 1.4 mm) and Ti in the Dore catchment; around 60 % of the variability in these elements was attributable to grain size (Veldkamp and Kroonenberg, 1993). Furthermore, in the Dore catchment concentrations of Zr also increased with decreasing median grain size (range 0.2-2.0 mm). In bed sediment samples from the Meurthe catchment, in the Vosges Mountains, France, Ti and Zr concentrations were higher in the <0.1 mm fraction than in the 0.1-0.3 mm and 0.3-0.5 mm fractions, and the distribution of Rb between the three fractions showed no consistent pattern (Albarède and Sehmi, 1995). Whitmore *et al.* (2004) found that the relationship between grain size and Ti, Rb and Zr in 27 New Guinea rivers draining to the Solomon Sea varied according to the underlying geology. Concentrations of these three elements tended to increase with decreasing grain size (gravel to mud) although in approximately half of cases there was no clear relationship (Whitmore *et al.*, 2004).

These studies of Zr, Ti and Rb distribution in fluvial sediments have generally focused on coarse-grained sediments, which are significantly coarser than the fine-grained overbank deposits in the Abermarlais floodplain. However, studies of variations in Zr, Ti and Rb concentrations between grain size fractions have also been undertaken in other depositional environments, such as lakes, in which finer-grained sediments predominate. For example, in samples recovered from the bed of Lake Nasser, Moalla (1997) found that Ti concentrations were highest in the 20-32 μm size fraction than in finer (<20 μm) or coarser (32-75 μm and >75 μm) fractions. Rb concentrations were found to be high in both the finest and coarsest fractions, which was attributed to the presence of Rb in clay minerals and as a detrital Rb-bearing phase in the coarse fraction (Moalla, 1997). In well-sorted surface sediments from the Skagerrak, Klaver and van Weering (1993) found that Rb was five times enriched in the clays relative to the sands whereas Zr was up to three times enriched in sands and silts compared with the clays. In a sample of modern mud from the Gulf of Mexico, Ti was found to be concentrated in the 2-10 μm fraction relative to the coarser (>10 μm) and finer (<2 μm) fractions. Rb concentrations were highest in the <2 μm fraction and considerably lower in the >10 μm fraction. Zr concentrations were highest in the >10 μm fraction and lowest

described by Jones *et al.* (2007), and was validated in the field during the coring programme (Figure 12).

The sites selected for sediment coring to produce the sedimentary flood records had a number of characteristics. First, they were located in palaeochannels as these topographic low points act as foci for deposition during overbank flood events through an extended period. Second, the sites were relatively close to the current channel but beyond the area of floodplain which has been reworked during the period for which historical maps and aerial photographs were available (c. 170-180 years). Parts of the floodplain which are distant from the present river channel may not have received appreciable amounts of sediment during flood events in recent centuries and consequently may produce a truncated record. Third, coring sites were selected where there was known, or expected, to be thick sequences of fine-grained, vertically-accreted floodplain deposits. In the Tywi catchment, the Abermarlais site was selected for production of a sedimentary flood record in preference to the other sites investigated because initial coring indicated that the thicknesses of fine-grained sediment were greater at this site than at the others. In addition, based on previous experience in the Severn and Dee catchments, this site was expected to be more suitable as the sediment was finer-grained (mainly silts and clays) than at other sites downstream (such as College Farm, where sedimentary sequences contained a higher proportion of sands, derived from the Old Red Sandstone, which crops out in the southern part of the catchment).

5.3.2 Sediment coring

Coring of floodplain sediment sequences was undertaken using a motorised percussion corer. Cores were collected from the Abermarlais site in June 2010. Initially, cores were collected using an open chamber gouge with an internal diameter of 75 mm. Cores were extracted in one metre sections and described in terms of colour, grain size distribution, bedding structures (e.g. imbrication) and organic matter content. Organic samples suitable for radiocarbon dating were collected where available. Subsequently, cased (50 mm diameter) cores were collected for detailed laboratory analysis. The tubes were sealed at each end immediately after extraction and were transported and stored in a horizontal position. Cased cores were initially split in half lengthwise using a circular saw to cut through the plastic tubing and either a wire or brass plates were used to split the sediment core into two halves. One half of the sample was designated as the archive half and was prepared for scanning using the Itrax core scanner and subsequently stored. The other half of the split core was sub-sampled for particle size analysis.

Five organic matter samples suitable for radiocarbon dating were recovered from the Abermarlais site: two of wood, two of charred material and one of plant material. These were sent to Beta Analytic for dating. The radiocarbon ages were calibrated using OxCal version 4 (Bronk Ramsey, 2009) and the IntCal04 calibration curve (Reimer *et al.*, 2009).

5.3.3 Itrax core scanning

The Itrax core scanner is an automated scanning instrument (Croudace *et al.*, 2006) which produces three principal types of data output: high resolution (up to 100 μm) optical and radiographic images and elemental (XRF) profiles of split sediment cores. For the production of flood records from the Abermarlais floodplain sediment sequences the Itrax core scanner was used for XRF measurements of 28 elements at 500 μm intervals using a Mo-tube operated at 30 kV and 30 mA and a 10 s exposure time. The Itrax core scanner provides XRF results as element intensities rather than element concentrations. Log-ratios of these XRF intensities were used to produce flood records. The use of log-ratios of element intensities for analysis of XRF core scan data is recommended by Weltje and Tjallingii (2008) since these are related to log-ratios of

Since sediment grain size data are a type of compositional data (subject to the constant sum constraint), grain sizes were expressed as log-ratios in order to permit the application of standard statistical methods (Aitchison, 1982; Weltje and Tjallingii, 2008). It is not possible to calculate a log-ratio for two sediment grain-size fractions where the percentage of sediment in either of them is 0. For this reason, log-ratios involving fractions coarser than 3 ϕ were not calculated for either site, since sediment in this grain size range was not present in a number of the samples analysed.

Log-ratios of sediment grain size data were calculated for each pair of 0.5 ϕ size fractions smaller than 3 ϕ . The larger grain size fraction was always used as the numerator and the smaller grain size fraction as the denominator, as this should produce a positive correlation with the Zr/Ti and Zr/Rb ratios, if they are suitable for use as grain size proxies at this site, since Zr is expected to be concentrated in a coarser grain size fractions than either Ti or Rb, and therefore the Zr/Ti and Zr/Rb ratios are expected to increase with increasing grain size. A mean value of $\ln(\text{Zr/Ti})$ and $\ln(\text{Zr/Rb})$ was calculated for each subsample using the Itrax core scan data for the depth interval from which the subsample was taken. Pearson product-moment correlation was used to establish whether there was a relationship between sediment grain size and whether this relationship was of the expected form (i.e. positive). Correlation coefficients were calculated for each grain-size log-ratio with each of the two lithogenic element log-ratios. A significance level was calculated for each correlation coefficient. Correlation coefficients were calculated using grain size results from both the sedigraph and the laser granulometer, in order to determine whether there was a difference in the results according to the method used (Tables 3 to 6). Within the results tables significant correlations are highlighted. Correlations significant at the 5 % level are shaded green, those significant at the 1 % level are shaded yellow, those significant at the 0.1 % level are shaded orange and those significant at the 0.01 % level are shaded red.

Table 4: Pearson product-moment correlation between grain-size log-ratios calculated using data from the Sedigraph and Zr/Rb log-ratios for the 16 subsamples from the Abernethy cores. The larger grain size fraction (columns) is always the dividend; the smaller (rows) is the divisor. Correlations coefficients are shown above significance levels (in brackets)

	2.5-3.0	3.0-3.5	3.5-4.0	4.0-4.5	4.5-5.0	5.0-5.5	5.5-6.0	6.0-6.5	6.5-7.0	7.0-7.5	7.5-8.0	8.0-8.5	8.5-9.0	9.0-9.5	9.5-10.0
3.0-3.5															
3.5-4.0	0.1164 (0.3338)														
4.0-4.5	0.0839 (0.3787)	0.0163 (0.4762)													
4.5-5.0	0.3185 (0.1335)	0.0366 (0.4506)	0.0224 (0.4698)												
5.0-5.5	-0.1892 (0.7586)	-0.2416 (0.8163)	-0.5127 (0.9789)	-0.1327 (0.6744)											
5.5-6.0	-0.1679 (0.7328)	-0.2199 (0.7935)	-0.4769 (0.9691)	-0.0729 (0.5979)	0.1807 (0.2515)										
6.0-6.5	-0.0880 (0.6271)	-0.1405 (0.698)	-0.3239 (0.8895)	0.1945 (0.2526)	0.4522 (0.0393)	0.4596 (0.0367)									
6.5-7.0	-0.0265 (0.5388)	-0.0774 (0.6122)	-0.2047 (0.7766)	0.2507 (0.1937)	0.6427 (0.0036)	0.6836 (0.0018)	0.7886 (0.0001)								
7.0-7.5	0.0297 (0.4565)	-0.0202 (0.5297)	-0.0750 (0.6088)	0.3101 (0.1403)	0.7071 (0.0011)	0.7536 (0.0004)	0.7992 (0.00008)	0.6598 (0.0027)							
7.5-8.0	0.0807 (0.3832)	0.0335 (0.451)	0.0525 (0.4235)	0.3555 (0.1061)	0.7281 (0.0007)	0.7642 (0.0003)	0.7992 (0.0001)	0.7387 (0.0005)	0.00106 (0.00048)						
8.0-8.5	0.1003 (0.3559)	0.0533 (0.4222)	0.1020 (0.3535)	0.3648 (0.0998)	0.7512 (0.0004)	0.7806 (0.0002)	0.7992 (0.0001)	0.7387 (0.0005)	0.00040 (0.00008)	0.4447 (0.0422)					
8.5-9.0	0.1101 (0.3424)	0.0624 (0.4093)	0.1232 (0.3247)	0.3714 (0.0955)	0.7615 (0.0003)	0.7966 (0.0001)	0.7992 (0.0001)	0.7387 (0.0005)	0.00069 (0.00008)	0.05411 (0.05411)	0.1550 (0.2833)				
9.0-9.5	0.1109 (0.3413)	0.0651 (0.4054)	0.1308 (0.3146)	0.3494 (0.1104)	0.7357 (0.0006)	0.7613 (0.0003)	0.7992 (0.0001)	0.7387 (0.0005)	0.00150 (0.00015)	0.06127 (0.06127)	0.1991 (0.2299)	0.0511 (0.4255)			
9.5-10.0	0.1133 (0.3381)	0.0663 (0.4037)	0.1349 (0.3092)	0.3045 (0.1449)	0.7468 (0.0004)	0.7613 (0.0003)	0.7992 (0.0001)	0.7387 (0.0005)	0.00197 (0.00019)	0.3210 (0.1127)	0.1422 (0.2997)	0.0599 (0.4128)	0.0217 (0.4682)		
	0.1520 (0.287)	0.1058 (0.3482)	0.2599 (0.1655)	0.3725 (0.0948)	0.7983 (0.0001)	0.8324 (0.00003)	0.7565 (0.00035)	0.6755 (0.00204)	0.5743 (0.00999)	0.3557 (0.08818)	0.2677 (0.1581)	0.2304 (0.1954)	0.2275 (0.1984)	0.2354 (0.1901)	

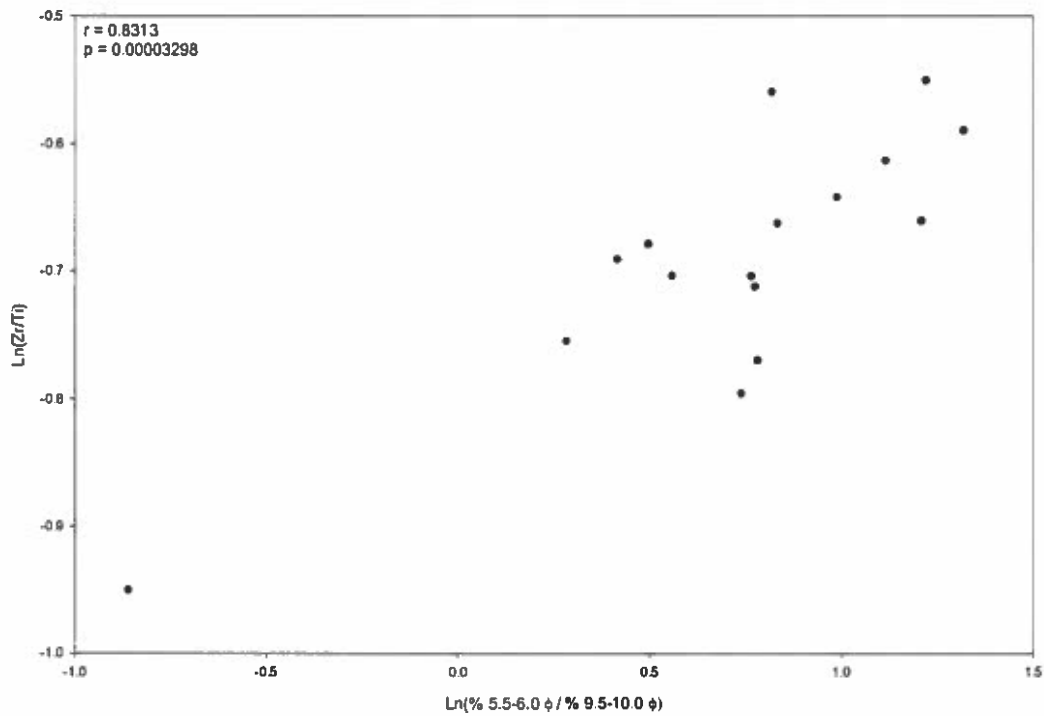


Figure 13: The most significant positive correlation between the log-ratio of Zr/Ti and sediment grain size (the ratio of the 5.5-6.0 ϕ fraction to the 9.5-10.0 ϕ fraction).

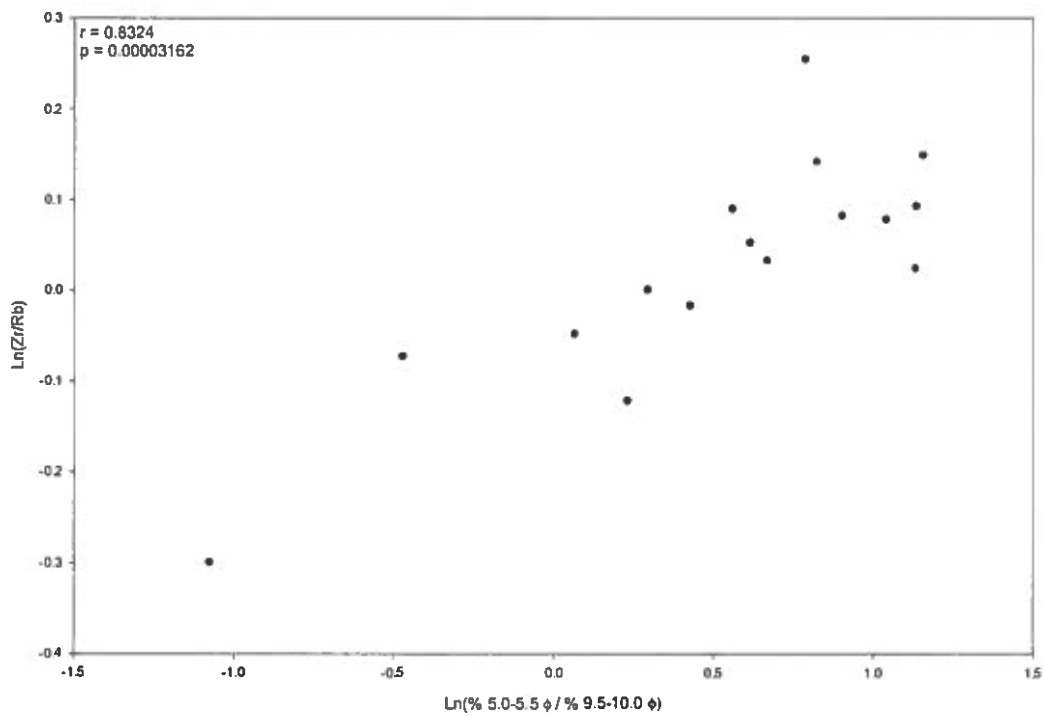


Figure 14: The most significant positive correlation between the log-ratio of Zr/Rb and sediment grain size (the ratio of the 5.5-6.0 ϕ fraction to the 9.5-10.0 ϕ fraction).

Table 6: Pearson product-moment correlation between grain-size log-ratios calculated using data from the laser granulometer and Zr/Rb log-ratios for the 16 subsamples from the Abermarlais cores. The larger grain size fraction (columns) is always the dividend; the smaller (rows) is the divisor. Correlations coefficients are shown above significance levels (in brackets).

	2.5-3.0	3.0-3.5	3.5-4.0	4.0-4.5	4.5-5.0	5.0-5.5	5.5-6.0	6.0-6.5	6.5-7.0	7.0-7.5	7.5-8.0	8.0-8.5	8.5-9.0	9.0-9.5
3.0-3.5														
3.5-4.0	0.0623 (0.3338)													
4.0-4.5	-0.033 (0.4513)	-0.0821 (0.5713)												
4.5-5.0	0.1294 (0.201)	-0.0976 (0.4792)	-0.0779 (0.3998)											
5.0-5.5	-0.2250 (0.673)	-0.2594 (0.7398)	-0.3574 (0.8194)	0.2374 (0.2492)										
5.5-6.0	-0.1586 (0.5767)	-0.1918 (0.6499)	-0.2494 (0.6866)	0.2486 (0.2407)	(0.07544)									
6.0-6.5	-0.0962 (0.489)	-0.1273 (0.5625)	-0.1327 (0.5342)	0.2646 (0.2316)	(0.07213)	(0.06862)								
6.5-7.0	-0.0510 (0.4307)	-0.0804 (0.502)	-0.0512 (0.4344)	0.2764 (0.2306)	(0.07069)	(0.06803)	(0.06822)							
7.0-7.5	-0.0238 (0.3999)	-0.0521 (0.4696)	-0.0049 (0.3851)	0.2852 (0.2344)	(0.06988)	(0.06787)	(0.06971)	0.4817 (0.0774)						
7.5-8.0	-0.0072 (0.3838)	-0.035 (0.4526)	0.0226 (0.3599)	0.2953 (0.2361)	(0.06762)	(0.06541)	(0.06746)	(0.07664)	(0.08971)					
8.0-8.5	0.0035 (0.3752)	-0.0238 (0.4435)	0.0403 (0.3462)	0.3082 (0.2337)	(0.06392)	(0.06093)	(0.06247)	(0.07411)	0.5445 (0.1011)	0.4908 (0.1562)				
8.5-9.0	0.0095 (0.373)	-0.0176 (0.4409)	0.0501 (0.3424)	0.3227 (0.2288)	0.4675 (0.0602)	(0.05659)	(0.05871)	(0.07932)	0.5110 (0.1412)	0.3924 (0.2529)	0.2592 (0.3906)			
9.0-9.5	0.0100 (0.3783)	-0.0168 (0.4462)	0.0509 (0.3504)	0.3371 (0.2237)	(0.05781)	(0.05457)	(0.06106)	0.5454 (0.109)	0.4138 (0.2428)	0.2576 (0.405)	0.1287 (0.5433)	0.0217 (0.658)		
9.5-10.0	0.0039 (0.3939)	-0.0229 (0.4622)	0.0404 (0.3751)	0.3510 (0.2204)	(0.05804)	0.5336 (0.0576)	(0.08032)	0.4551 (0.2088)	0.2568 (0.43)	0.1092 (0.5835)	0.0047 (0.6852)	-0.0787 (0.7625)	-0.1487 (0.8224)	
	-0.0166 (0.4342)	-0.0435 (0.5036)	0.0058 (0.4406)	0.3678 (0.2229)	(0.06504)	0.5330 (0.0805)	0.4624 (0.2001)	0.2158 (0.51)	0.0392 (0.6866)	-0.0577 (0.7625)	-0.1250 (0.8115)	-0.1797 (0.85)	-0.2253 (0.8801)	-0.2624 (0.9024)

This may be caused by changes at the site during the event, related to the flow of water or deposition of sediment in the immediate vicinity of the site from which the sediment sequence was recovered, or, perhaps more likely, to variations in the calibre of sediment supplied to the site relating to fluctuations in water depth and flow velocity as the result of, for example, the arrival at different times of minor peaks generated in different sub-catchments upstream of the site or the effects of a multi-peaked rainfall event. Therefore, a cluster of peaks in the record, which occur within a few millimetres or, in some cases, a few centimetres of each other, and between which levels of the log-ratios are in general elevated above the norm, are interpreted as representing sediment deposited during the course of a single flood event.

It has thus far not been possible to determine the exact extent to which the magnitudes of peaks in the records of these geochemical grain size proxies is related to the peak discharges of the floods that deposited the sediment. The assumption is here made that a peak in either or both of $\ln(\text{Zr/Rb})$ and $\ln(\text{Zr/Ti})$ indicates that a major flood event has occurred. It is also assumed that, to a certain extent, the relative magnitudes of the peaks within these data series reflect the relative magnitudes of the floods that they record. However, it has not been possible to determine either the magnitude of the errors which might be expected when using the Itrax core scanner to measure the variation in elemental concentrations or the magnitude of the errors between the grain size as represented as represented by the proxy and the actual grain size or the magnitude of the errors which would result in estimating the magnitude of a flood peak discharge from the sediment which it deposited. Notwithstanding this, it has been possible to demonstrate at a site in the Severn catchment (the Roundabout, north of Welshpool), by comparison of the grain size proxy record with the occurrence of isolated individual layers of gravel within the predominantly silty sediment sequence analysed, that the coarsest layers within the sediment sequence produced the largest peaks in the grain size proxy record. The assumption that such coarse layers were deposited during flood events the magnitude of which is represented by the calibre of the sediment is an assumption which underpins the field of palaeoflood hydrology.

two cores from Abermarlais to a time scale: the ground surface was assigned an age of AD2010, the year in which the cores were collected from the floodplain. Three radiocarbon-dated samples were available for Core AM1. The upper two radiocarbon samples returned ages which were very similar, as were also the calibrated ranges of these dates. Therefore, a mean depth for the two samples was calculated and the midpoint of the 2σ ages was used in this case. The depth and mid-point of the 2σ calibrated age range for the third sample from close to the base of the cored sequence (below the base of the sediment sequence which was recovered for laboratory analysis) was for the depth – time conversion of the basal portion of the sequence. Two radiocarbon-dated samples were available for Core AM3, both of which were recovered from horizons below those for which sediment had been recovered for laboratory analysis. The upper (and slightly older) of these two samples was used for the depth – time conversion of this core.

Linear interpolation between the dated horizons was used estimate the age of each Zr/Rb or Zr/Ti measurement within the record. For Core AM1 therefore, two different sedimentation rates were calculated, for the upper and lower portions of the core (above and below 1560 mm). For Core AM3 a single sedimentation rate was assumed for the entire period of record. The use of linear interpolation to estimate the ages of floodplain sediments between such a small number of dated horizons is not ideal. Work in other catchments, notably the upper River Severn, has revealed the extent to which floodplain sedimentation rates may vary, particularly due to anthropogenic activity in recent centuries. This includes expansion of areas used for agriculture, particularly into upland parts of the catchment and discharge of fine-grained mine waste directly to the river system. The latter is not likely to be as significant in the upper Tywi catchment as it was in the upper Severn during the 1860s to 1890s, but the extent to which agricultural activities may have affected sedimentation rates, and therefore the estimated ages of major flood events within the records from the Tywi catchment is unknown. This must be borne in mind when interpreting the result presented in the following section.

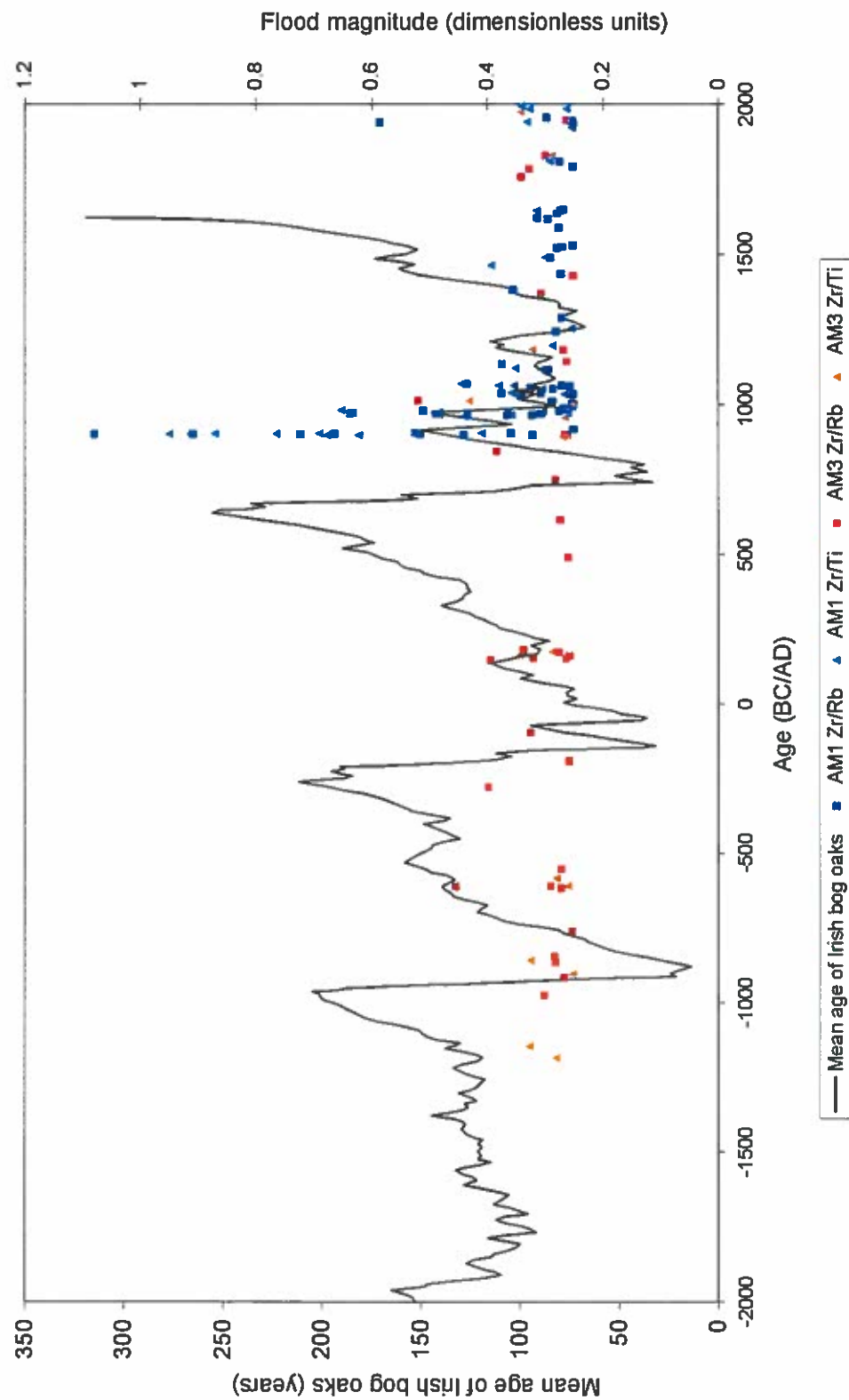


Figure 16: Flood peaks derived from the Zr/Ti and Zr/Rb records from Cores AM1 and AM3 plotted against the mean age of Irish bog oaks (Leuschner *et al.*, 2002).

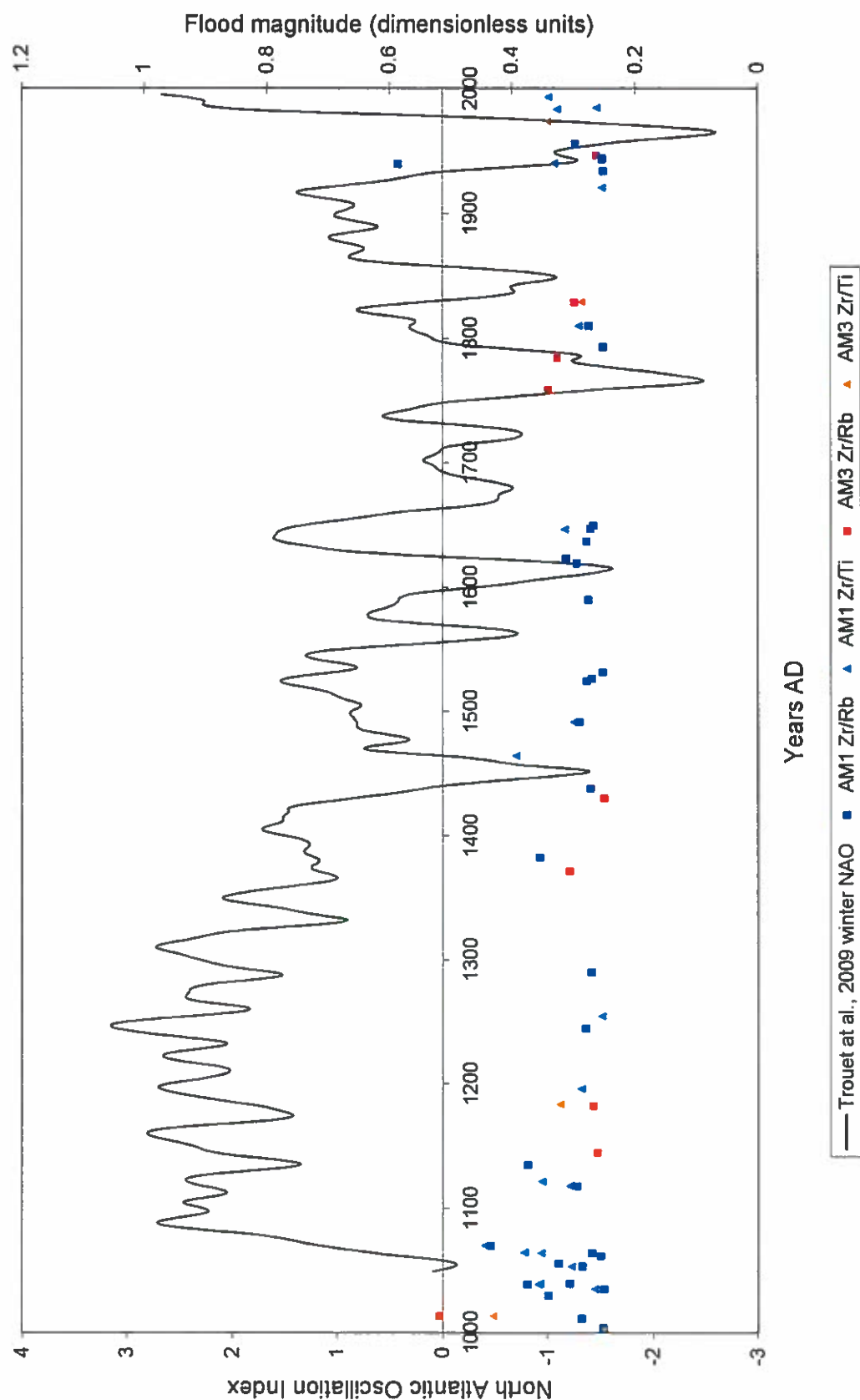


Figure 17: Flood peaks derived from the Zr/Ti and Zr/Rb records from Cores AM1 and AM3 plotted against reconstructed North Atlantic Oscillation Index (Trouet *et al.*, 2009).

affected the sedimentary sequences which are used as a record of flood events. Other issues relate to interpretation of the variation in the geochemical grain size proxies, in particular, the extent to which this reflects flood peak discharges. This is a broader issue relating to the reconstruction of palaeoflood records from fine-grained floodplain sediment sequences and may be addressed by future research.

- Driese, S. G., Li, Z.-H. and Horn, S. P., (2005). Late Pleistocene and Holocene climate and geomorphic histories as interpreted from a 23,000 14C yr B.P. paleosol and floodplain soils, southeastern West Virginia. *Quaternary Research*, **63**, 136-149.
- Dunne, T. and Leopold, L. B., (1978). *Water in Environmental Planning*. W. H. Freeman, New York.
- Dypvik, H. and Harris, N. B., (2001). Geochemical facies analysis of fine-grained siliciclastics using Th/U, Zr/Rb and (Zr+Rb)/Sr ratios. *Chemical Geology*, **181**, 131-146.
- Ely, L. L., Enzel, Y., Baker, V. R. and Cayan, D. R., (1993). A 5000-year record of extreme floods and climate change in the southwestern United States. *Science*, **262**, 410-412.
- Environment Agency, (2010). *HiFlows-UK* [online]. Environment Agency. Available from: <http://www.environment-agency.gov.uk/hiflows/91727.aspx> [Accessed: 2010].
- Frost, J. R. and Jones, E. C., (1989). The October 1987 flood on the River Tywi. In: Institute of Hydrology (ed.) *Hydrological Data United Kingdom 1987 Yearbook*. Institute of Hydrology, Wallingford. 23-30.
- Goman, M. and Leigh, D. S., (2004). Wet early to middle Holocene conditions on the upper Coastal Plain of North Carolina, USA. *Quaternary Research*, **61**, 256-264.
- Gumbel, E. J., (1958). *Statistics of Extremes*. Columbia University Press, New York.
- Hardardóttir, J., Geirsdóttir, Á. and Sveinbjörnsdóttir, Á. E., (2001). Seismostratigraphy and sediment studies of Lake Hestvatn, southern Iceland: implications for the deglacial history of the region. *Journal of Quaternary Science*, **16**, 167-179.
- Hayashi, K.-I., Fujisawa, H., Holland, H. D. and Ohmoto, H., (1997). Geochemistry of ~1.9 Ga sedimentary rocks from northeastern Labrador, Canada. *Geochimica et Cosmochimica Acta*, **61**, 4115-4137.
- Jain, S. and Lall, U., (2000). Magnitude and timing of annual maximum floods: Trends and large-scale climatic associations for the Blacksmith Fork River, Utah. *Water Resources Research*, **36**, 3641-3651.
- Jain, S. and Lall, U., (2001). Floods in a changing climate: Does the past represent the future? *Water Resources Research*, **37**, 3193-3205.
- Jones, A. F., Brewer, P. A., Johnstone, E. and Macklin, M. G., (2007). High-resolution geomorphological mapping of river valley environments using airborne LiDAR data. *Earth Surface Processes and Landforms*, 1574-1592.
- Karathanasis, A. D. and Macneal, B. R., (1994). Evaluation of parent material uniformity criteria in loess-influenced soils of west-central Kentucky. *Geoderma*, **64**, 73-92.
- Kidson, R. and Richards, K. S., (2005). Flood frequency analysis: assumptions and alternatives. *Progress in Physical Geography*, **29**, 392-410.
- Klaver, G. T. and van Weering, T. C. E., (1993). Rare Earth Element fractionation by selective sediment dispersal in surface sediments: the Skagerrak. *Marine Geology*, **111**, 345-359.
- Knox, J. C., (1987). Stratigraphic evidence of large floods in the upper Mississippi Valley. In: Mayer, L. and Nash, D. (eds.) *Catastrophic Flooding*. Allen and Unwin, Winchester, MA. 155-180.

Oh, N.-H. and Richter, D. D., (2005). Elemental translocation and loss from three highly weathered soil-bedrock profiles in the southeastern United States. *Geoderma*, **126**, 5-25.

Oldfield, F., Wake, R., Boyle, J., Jones, R., Nolan, S., Gibbs, Z., Appleby, P., Fisher, E. and Wolff, G., (2003). The late-Holocene history of Gormire Lake (NE England) and its catchment: a multiproxy reconstruction of past human impact. *The Holocene*, **13**, 677-690.

Reimann, C. and de Caritat, P., (1998). *Chemical Elements in the Environment: Factsheets for the Geochemist and Environmental Scientist*. Springer-Verlag, Berlin.

Reimer, P. J., Baillie, M. G. L., Bard, E., Bayliss, A., Beck, J. W., Blackwell, P. G., Bronk Ramsey, C., Buck, C. E., Burr, G. S., Edwards, R. L., Friedrich, M., Grootes, P. M., Guilderson, T. P., Hajdas, I., Heaton, T. J., Hogg, A. G., Hughen, K. A., Kaiser, K. F., Kromer, B., McCormac, F. G., Manning, S. W., Reimer, R. W., Richards, D. A., Southon, J. R., Talamo, S., Turney, C. S. M., van der Plicht, J. and Weyhenmeyer, C. E., (2009). IntCal09 and Marine09 radiocarbon calibration curves, 0-50,000 years cal BP. *Radiocarbon*, **51**, 1111-1150.

Rose, A. W., Hawkes, H. E. and Webb, J. S., (1979). *Geochemistry in Mineral Exploration*. 2nd edition. Academic Press, New York.

Scheffler, K., Buehmann, D. and Schwark, L., (2006). Analysis of late Palaeozoic glacial to postglacial sedimentary successions in South Africa by geochemical proxies - Response to climate evolution and sedimentary environment. *Palaeogeography Palaeoclimatology Palaeoecology*, **240**, 184-203.

Schneider, R. R., Price, B., Müller, P. J., Kroon, D. and Alexander, I., (1997). Monsoon related variations in Zaire (Congo) sediment load and influence of fluvial silicate supply on marine productivity in the east equatorial Atlantic during the last 200,000 years. *Paleoceanography*, **12**, 463-481.

Sheffer, N. A., Rico, M., Enzel, Y., Benito, G. and Grodek, T., (2008). The palaeoflood record of the Gardon River, France: a comparison with the extreme 2002 flood event. *Geomorphology*, **98**, 71-83.

Shotyk, W., Weiss, D., Kramers, J. D., Frei, R., Cheburkin, A. K., Gloor, M. and Reese, S., (2001). Geochemistry of the peat bog at Etang de la Gruère, Jura Mountains, Switzerland, and its record of atmospheric Pb and lithogenic trace metals (Sc, Ti, Y, Zr, and REE) since 12,370 ¹⁴C yr BP. *Geochimica et Cosmochimica Acta*, **65**, 2337-2360.

Stone, P., Green, P. M. and Williams, T. M., (1997). Relationship of source and drainage geochemistry in the British paratectonic Caledonides - an exploratory regional assessment. *Transactions of the Institution of Mining and Metallurgy Section B - Applied Earth Science*, **106**, B79-B84.

Sudom, M. D. and St. Amand, R. J., (1971). Use of quartz, zirconium and titanium as indices in pedological studies. *Canadian Journal of Soil Science*, **51**, 385-396.

Sutherland, R. A., (2000). A comparison of geochemical information obtained from two fluvial bed sediment fractions. *Environmental Geology*, **39**, 330-341.

Thorndycraft, V. R., Hu, Y., Oldfield, F., Crooks, P. R. J. and Appleby, P. G., (1998). Individual flood events detected in the recent sediments of the Petit Lac d'Annecy, eastern France. *The Holocene*, **8**, 741-746.

Veldkamp, A. and Kroonenberg, S. B., (1993). Application of bulk sand geochemistry in mineral exploration and Quaternary research: a methodological study of the Allier and Dore terrace sands, Limagne rift valley, France. *Applied Geochemistry*, **8**, 177-187.